

A model explaining neutrino masses and the DAMPE cosmic ray electron excess

Yi-Zhong Fan^{a,b*}, Wei-Chih Huang^{c†}, Martin Spinrath^{d‡}, Yue-Lin Sming Tsai^{e§}, and Qiang Yuan^{a,b¶}

^aKey Laboratory of Dark Matter and Space Astronomy,

Purple Mountain Observatory, Chinese Academy of Sciences, Nanjing 210008, China

^bSchool of Astronomy and Space Science, University of Science and Technology of China, Hefei, Anhui 230026, China

^cCP³ Origins, University of Southern Denmark, Campusvej 55, DK-5230 Odense M, Denmark

^dPhysics Division, National Center for Theoretical Sciences, Hsinchu 30013, Taiwan

^eInstitute of Physics, Academia Sinica, Nangang, Taipei 11529, Taiwan

We propose a flavored $U(1)_{e\mu}$ neutrino mass and dark matter (DM) model to explain the recent DArk Matter Particle Explorer (DAMPE) data, which feature an excess on the cosmic ray electron plus positron flux around 1.4 TeV. Only the first two lepton generations of the Standard Model are charged under the new $U(1)_{e\mu}$ gauge symmetry. A vector-like fermion ψ , which is our DM candidate, annihilates into e^\pm and μ^\pm via the new gauge boson Z' exchange and accounts for the DAMPE excess. We have found that the data favors a ψ mass around 1.5 TeV and a Z' mass around 2.6 TeV, which can potentially be probed by the next generation lepton colliders and DM direct detection experiments.

PACS numbers:

I. INTRODUCTION

The newly released data from the DArk Matter Particle Explorer (DAMPE [1]) exhibits an intriguing excess of the cosmic ray electron plus positron (hereafter CRE) flux at energies around 1.4 TeV [2]. We provide here a dark matter (DM) explanation based on a simple flavored $U(1)$ extension of the standard model (SM). This kind of extension is known for quite a while [3–5]. Well-studied scenarios are those involving the second and third generation, $U(1)_{\mu\tau}$ (denoted as $L_\mu - L_\tau$ in the literature), which are partially motivated by the large mixing angle inferred from atmospheric neutrino oscillations [6–8]. Such models are recently used to explain anomalies in Higgs and quark flavor physics (see, e.g. [9–12]). This class of models was also discussed in the context of the PAMELA, ATIC and FERMI results [13].

In this work, we focus on another variant, $U(1)_{e\mu}$, under which only the first two generation leptons are charged. This choice is inspired by DAMPE CRE data as we are trying to establish the connection between the DM explanation for the CRE excess and the neutrino mass generation mechanism. In this framework, the DM candidate is a vector-like fermion ψ whose stability is guaranteed by an accidental $U(1)$ symmetry. The DM annihilation into e^\pm and μ^\pm (also ν_e and ν_μ) can account well for the DAMPE excess. Since the generated electrons and positrons lose energies quickly on the way to the Earth, the CREs detected by DAMPE must come from regions close to the solar neighborhood. As a result, we assume that there exists a nearby DM subhalo, which is also predicted by the structure formation of the cold DM scenario (e.g. [14, 15]).

II. THE MODEL

Our model is a rather minimal extension of the SM. We add one additional anomaly-free $U(1)_{e\mu}$ gauge group, two additional scalars, ϕ_1 and ϕ_2 , whose vacuum expectation values (vevs) break the new $U(1)_{e\mu}$ spontaneously, three right-handed neutrinos, and a vector-like fermion ψ as a DM candidate. Only the lepton doublets, right-handed leptons and neutrinos of the first two

TABLE I: Charge assignments of the fields under the new $U(1)_{e\mu}$ gauge group which is broken by the vevs of the scalar fields ϕ_1 and ϕ_2 . The fermion ψ is our DM candidate. These three new fields do not carry any SM quantum numbers and all the SM fields not shown are neutral under $U(1)_{e\mu}$.

Field	L_e	L_μ	e_R	μ_R	N_1	N_2	N_3	ψ	ϕ_1	ϕ_2
$U(1)_{e\mu}$ charge	1	-1	1	-1	1	-1	0	q_ψ	1	2

* E-mail: yzfan@pmo.ac.cn

† E-mail: huang@cp3.sdu.dk

‡ E-mail: martin.spinrath@cts.nthu.edu.tw

§ E-mail: smingtsai@gate.sinica.edu.tw

¶ E-mail: yuanq@pmo.ac.cn

generations are charged under $U(1)_{e\mu}$ as summarized in Table I. The fermion ψ is stable since the Lagrangian carries an additional accidental $U(1)$ symmetry which can be interpreted as ψ -number.

In this model, the $U(1)_{e\mu}$ symmetry demands both the charged lepton and the neutrino Yukawa couplings to be diagonal in the flavor basis. On the other hand, when the scalars receive a vev the resulting right-handed neutrino mass matrix is an unconstrained symmetric matrix:

$$M_R = \frac{1}{2} \begin{pmatrix} y_{11}\langle\phi_2^*\rangle & M_{12} & y_{13}\langle\phi_1^*\rangle \\ M_{12} & y_{22}\langle\phi_2\rangle & y_{23}\langle\phi_1\rangle \\ y_{13}\langle\phi_1^*\rangle & y_{23}\langle\phi_1\rangle & M_3 \end{pmatrix}, \quad (1)$$

where y_{ij} are Yukawa couplings of the right-handed neutrinos with the scalar singlets ϕ_1 and ϕ_2 , and M_{12} and M_3 are mass parameters. With such structures we can reproduce the neutrino masses and mixing angles via the Type-I seesaw mechanism.

The scalar potential in the unbroken phase reads

$$V_s = -\mu_H^2 |H|^2 + \lambda_H |H|^4 - \mu_{\phi_i}^2 |\phi_i|^2 + \lambda_i |\phi_i|^4 + \lambda_{12} |\phi_1|^2 |\phi_2|^2 + \kappa_i |\phi_i|^2 |H|^2, \quad (2)$$

where H is the usual SM Higgs doublet, and we have $\mu_H^2 > 0$ and $\mu_{\phi_i}^2 > 0$ for $i = 1, 2$. After electroweak and $U(1)_{e\mu}$ symmetry breaking, $\langle H^0 \rangle = v_H / \sqrt{2}$ and $\langle \phi_i \rangle = v_{\phi_i} / \sqrt{2}$, there exist three physical CP even Higgs bosons h and η_i with masses m_h and m_{η_i} , and one CP odd Higgs boson ζ with a mass m_ζ . For simplicity, we assume here that the κ_i are negligibly small so that h is identified with the SM Higgs boson. The κ_i terms could be probed with future Higgs precision data. A careful and detailed study is, however, beyond the scope of this work.

The mass of the new gauge boson is $m_{Z'}^2 = g_{e\mu}^2 (v_1^2 + 4v_2^2)$ on tree level, where $g_{e\mu}$ is the $U(1)_{e\mu}$ gauge coupling. Since the ϕ_i do not carry any SM quantum numbers, the masses of the SM gauge bosons are not affected by $\langle \phi_i \rangle$ on tree level.

The relevant Lagrangian for the DM annihilation into SM fermions f is

$$\begin{aligned} \mathcal{L} \supset & -\frac{1}{2} m_{Z'}^2 Z'^\mu Z'_\mu - m_\psi \bar{\psi} \psi + i q_\psi g_{e\mu} \bar{\psi} \gamma^\mu \psi Z'_\mu \\ & - \sum_{f=e,\mu} (m_f \bar{f} f - i q_f g_{e\mu} \bar{f} \gamma^\mu f Z'_\mu) \\ & + \sum_{f=\nu_e, \nu_\mu} i q_f g_{e\mu} \bar{f} \gamma^\mu \left(\frac{1 - \gamma_5}{2} \right) f Z'_\mu, \end{aligned} \quad (3)$$

where q_f labels the $U(1)_{e\mu}$ charge of the field f , c.f. Table I. The SM fermion masses are neglected due to $m_f \ll m_\psi$ for our regions of interest. We further assume that the extra scalars, η_i and ζ , and the right-handed neutrinos are all heavier than ψ and Z' .

The DM annihilation cross-section into a SM fermion pair $\bar{f}f$, $\sigma(\bar{\psi}\psi \rightarrow Z' \rightarrow \bar{f}f)$, multiplied by the DM relative velocity v_{rel} , is

$$\sigma v_{\text{rel}} = c_f \frac{q_\psi^2 q_f^2 g_{e\mu}^4 (s + 2m_\psi^2)}{6\pi \left[(s - m_{Z'}^2)^2 + m_{Z'}^2 \Gamma_{Z'}^2 \right]}, \quad (4)$$

where $c_f=1$ (1/2) for e and μ (ν_e and ν_μ), and $s = 16m_\psi^2 / (4 - v_{\text{rel}}^2)$ is the square of the center-of-mass energy. Note that σv_{rel} is dominated by the s -wave component as $v_{\text{rel}} \rightarrow 0$. The total Z' decay width into $\bar{f}f$ and $\bar{\psi}\psi$ reads

$$\begin{aligned} \Gamma_{Z'} = & \sum_{f=e,\mu,\nu_e,\nu_\mu} c_f \frac{q_f^2 g_{e\mu}^2 m_{Z'}}{12\pi} \\ & + \Theta(m_{Z'} - 2m_\psi) \frac{q_\psi^2 g_{e\mu}^2 \sqrt{m_{Z'}^2 - 4m_\psi^2} (m_{Z'}^2 + 2m_\psi^2)}{12\pi m_{Z'}^2}. \end{aligned} \quad (5)$$

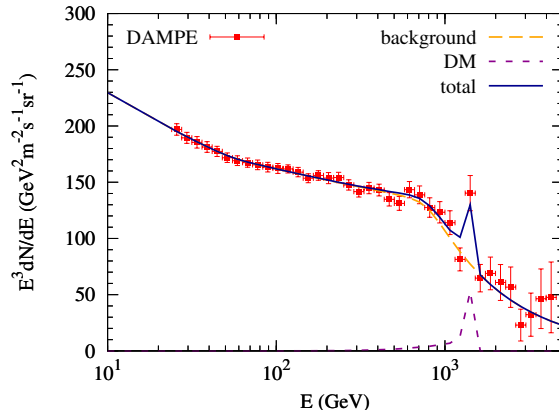


FIG. 1: Illustration of the fit to the total DAMPE CRE flux with the background and the DM contribution.

III. PARAMETER SPACE

We first study the CRE background, i.e., the CRE not from DM annihilations. The background component (from astrophysical sources such as supernova remnants and/or pulsars) is assumed to have a double-broken power-law form as

$$\Phi_{\text{bkg}} = \Phi_0 E^{-\gamma} \left[1 + \left(\frac{E_{\text{br},1}}{E} \right)^\delta \right]^{\Delta\gamma_1/\delta} \left[1 + \left(\frac{E}{E_{\text{br},2}} \right)^\delta \right]^{\Delta\gamma_2/\delta}, \quad (6)$$

with the first break at $E_{\text{br},1} \sim 50$ GeV and the second one at $E_{\text{br},2} \sim 900$ GeV according to the Fermi-LAT [16] and DAMPE observations [2]. During the analysis, we fix $E_{\text{br},1}$ to 50 GeV, and the sharpness parameter δ to 10. The fit to the DAMPE data with the e^\pm energy between 25 GeV and 4.6 TeV without taking into account the peak (excess) leads to $\Phi_0 = 247.2$ $\text{GeV}^{-1} \text{m}^{-2} \text{s}^{-1} \text{sr}^{-1}$, $\gamma = 3.092$, $\Delta\gamma_1 = 0.096$, $\Delta\gamma_2 = -0.968$, and $E_{\text{br},2} = 885.4$ GeV.

Next, we include the contribution from a nearby DM subhalo in addition to the background and fit again to the data. The density distribution inside the subhalo is assumed to be a Navarro-Frenk-White profile [17], with a truncation at the tidal radius r_t [18]. For the determination of the density profile of the subhalo, we refer to Ref. [19]. As for the propagation of electrons and positrons in the Milky Way, we adopt the Green's function approach presented in Ref. [20].

The background parameters $E_{\text{br},2}$ and $\Delta\gamma_2$ are correlated to the DM component, and thus are being varied in the fit. Other parameters are fixed to the best-fit values obtained in the aforementioned background-only fit. Fig. 1 shows the model prediction of the CRE flux for $m_\psi = 1.54$ TeV, $\langle\sigma v_{\text{rel}}\rangle = 6.82 \times 10^{-25} \text{cm}^3 \text{s}^{-1}$, and the DM subhalo with a mass of $M_{\text{sub}} = 1.25 \times 10^6 M_\odot$ at a distance of $d = 0.1$ kpc from the Earth.

There are four relevant DM parameters in this model: m_ψ , $m_{Z'}$, $g_{e\mu}$, and q_ψ . To ensure the DM model withstands various experimental bounds and to explore favored regions of the parameter space, we consider the constraints from (i) the relic density, (ii) the cosmic microwave background (CMB), (iii) the LEP measurements on the cross-sections of the leptonic final states, (iv) DM direct detection, and (v) the DAMPE data. Note that the recent measurements of the CRE flux by the Calorimetric Electron Telescope (CALET) up to 3 TeV [21] are not considered here, because of the relatively large statistical and systematic uncertainties. For the relic density, we use the Planck result: $\Omega_\psi h^2 = 0.1199 \pm 0.0027$ [22] plus 10% theoretical uncertainties, which are commonly included to take into account the discrepancies among the different Boltzmann equation solvers and entropy tables.

The constraints on the DM annihilation rate from the PLANCK TT, TE, EE+LowP power spectra (Table 6 of Ref. [22]) are employed. Moreover, the LEP measurements on the cross-section of $e^+e^- \rightarrow \ell^+\ell^-$ can be translated into constraints on the new physics scale in the context of the effective four-fermion interactions [23]

$$\mathcal{L}_{\text{eff}} = \frac{4\pi}{(1+\delta)\Lambda^2} \sum_{i,j=L,R} \eta_{i,j} \bar{e}_i \gamma_\mu e_i \bar{f}_j \gamma^\mu f_j, \quad (7)$$

where $\delta = 0$ (1) for $f \neq e$ ($f = e$), and $\eta_{ij} = 1$ (-1) corresponds to constructive (destructive) interference between the SM and new physics processes. For $e^+e^- \rightarrow e^+e^-$ ($e^+e^- \rightarrow \mu^+\mu^-$), one has $\Lambda = 18$ (21.7) TeV, which implies $m_{Z'}/g_{e\mu} \gtrsim 7.2$ (6.1) TeV.

Even if DM couples only to leptons at tree level, spin-independent DM-proton interactions can still be loop-induced and probed as discussed in, for instance, Refs. [24–26]. A recent updated analysis based on a leptophilic dark sector in Ref. [26] attains the constraints from direct detection on the DM and mediator mass for different types of DM-lepton interactions, as

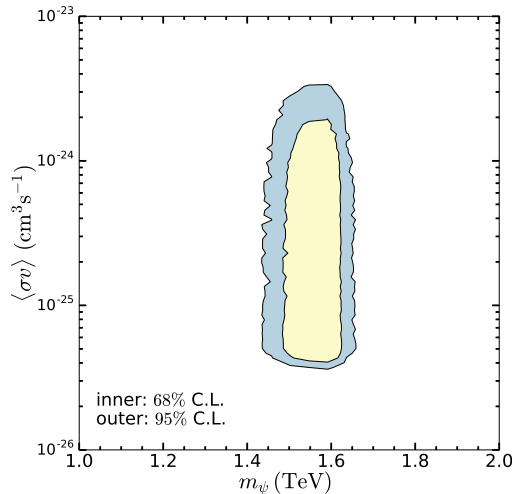


FIG. 2: The 68% (inner) and 95% (outer) contours for m_ψ versus $\langle\sigma v_{\text{rel}}\rangle$. The total likelihoods included here are the relic density, the CMB constraints on DM annihilation into charged leptons, the LEP Z' constraints, the DM direct detection constraints and the DAMPE CRE measurement.

displayed in Fig. 2 therein. To apply the results to our model, we take the direct detection constraints in Ref. [26] for the vector-type interaction (solid blue line in their upper-right panel of Fig. 2) and then rescale it with our coupling constants. To realize our $U(1)_{e\mu}$ model, only the vector couplings for e and μ are nonzero, $g_{Ve}, g_{V\mu} \neq 0$ in the notation of Ref. [26]. Furthermore, the direct detection limit given in Ref. [26] is based on the LUX WS2014-16 run [27] which is slightly less stringent than that from the latest PandaX-II data [28]. As a consequence, with the new data the lower bound on the mediator mass will improve by a factor of $[\sigma_{\chi p}^{\text{SI}}(\text{LUX})/\sigma_{\chi p}^{\text{SI}}(\text{PandaX})]^{1/4}$, given a DM mass. With these rescalings taken into account, the derived bound for $m_{Z'} \sim \mathcal{O}(\text{TeV})$ is

$$g_{e\mu}^2 q_\psi \left(\frac{1170 \text{ GeV}}{m_{Z'}} \right)^2 \lesssim 1, \quad (8)$$

where we set $q_{e,\mu} = 1$. The XENON1T [29] data yield a similar limit.

The DM particle mass m_ψ in the analysis ranges from 0.5 to 5.0 TeV with the Z' mass in the range $m_\psi < m_{Z'} < 2m_\psi$, making the current $\langle\sigma v_{\text{rel}}\rangle$ larger than it was at the time of DM freeze-out, although the resonance enhancement needs not to be enormous. The DM charge q_ψ is varied between 0.5 and 5. We conducted a random scan and a Nest-Sampling scan of the parameter space. After identifying the high probability region by checking the result of the random scan, we utilized MultiNest [30] in the Nest-Sampling scan to optimize the coverage of sampling. The two scans ($\sim 10^8$ points) are then combined with a profile likelihood method.

In Fig. 2 and Fig. 3, we present the 68% (inner) and 95% (outer) profile likelihood contours on the plane of $m_\psi - \langle\sigma v_{\text{rel}}\rangle$ and $m_\psi - m_{Z'}$, respectively. The preferred DM mass region is between 1.4 TeV and 1.7 TeV with a Z' mass between 1.9 TeV and 3.2 TeV and $g_{e\mu}$ between 0.014 and 0.38 at the 95% CL. We find no preferred region for q_ψ over the scan range [0.5, 5].

Together with the coupling limits from PLANCK (relic density and CMB), the DM annihilation cross-section is confined within $[3 \times 10^{-26}, 3 \times 10^{-24}] \text{ cm}^3 \text{ s}^{-1}$ as shown in Fig. 2. The annihilation cross-section is inversely proportional to the mass of the subhalo, which is restricted inside the range of $[2.5 \times 10^5, 6 \times 10^7] M_\odot$, assuming a distance of $d = 0.1 \text{ kpc}$. For different values of d , the required subhalo mass scales approximately as d^2 [19].

IV. OTHER CONSTRAINTS AND PROSPECTS

We further consider bounds from DM indirect detection, and also comment on the model's detectability at future DM direct detection and lepton colliders.

- Fermi-LAT γ -ray data

We have checked that the inverse Compton emission from the diffuse electrons and positrons for the presumed subhalo is negligibly small. On the other hand, we also study the γ -ray emission produced via the internal bremsstrahlung process

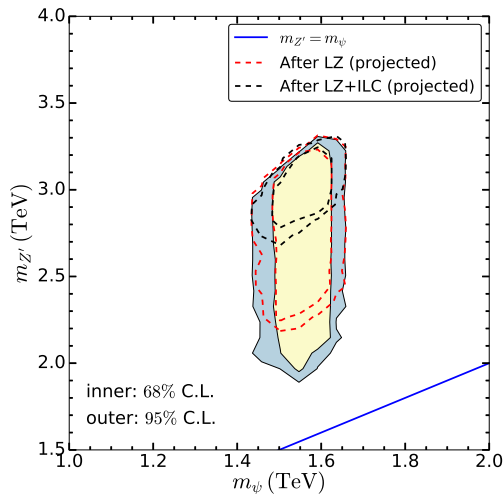


FIG. 3: The 68% (inner) and 95% (outer) contours for m_ψ versus $m_{Z'}$. The filled contours are based on the present constraints as shown in Fig. 2. However, for a future prospect, including the projected constraints from LZ (red dashed contours) and LZ+ILC (black dashed contours) are presented as well.

by the charged fermions which come from the Z' decays. The process is known as the final state radiation (FSR; [31]). The FSR γ -rays from the subhalo are essentially extended over a considerable patch of the sky. The expected numbers of photons from the DM annihilation within the subhalo for $E_\gamma > 100$ GeV are estimated to be 0.7, 2.0, 5.9, 13.6, 25.3, 34.1, 34.4, for the integral radius of 0.1° , 0.3° , 1° , 3° , 10° , 90° , 180° respectively around the halo center, assuming an exposure of 3×10^{11} $\text{cm}^2 \text{s}$ for ten years of operation of the Fermi-LAT. The corresponding numbers of the extragalactic background photon emission, according to the Fermi-LAT measurements [32], are 0.001, 0.01, 0.1, 1.1, 11.8, 776.6, and 1553.2, respectively. If the center of the subhalo is located in the inner Galaxy direction, the corresponding diffuse background could be higher by 10 – 100 times [33]. It implies that the detection of the γ -ray emission from such a subhalo is challenging (and hence unconstrained) to the Fermi-LAT in light of the small number of photons and a very long exposure time. The future ground based Cherenkov Telescope Array (CTA; [34]) may be able to detect such an extended γ -ray source and test our model.

The Fermi-LAT γ -ray observations of the Milky Way halo set an upper limit of $\langle \sigma_{\text{vrel}} \rangle \lesssim 5 \times 10^{-24} \text{ cm}^3 \text{ s}^{-1}$ for $m_\psi \sim 1.5$ TeV, presuming Majorana DM which annihilates into $\mu^+ \mu^-$ only. The DAMPE-favored parameter region is completely free from this constraint.

- IceCube ν data

The IceCube observations of neutrinos from the Galactic center region give upper limits on the DM annihilation cross-sections (again assuming Majorana DM) of $9.6 \times 10^{-23} \text{ cm}^3 \text{ s}^{-1}$ and $2.6 \times 10^{-22} \text{ cm}^3 \text{ s}^{-1}$ for the $\mu^+ \mu^-$ and $\nu \bar{\nu}$ channels, respectively [35]. These values are much larger than what is required to explain the DAMPE data, and no constraints can be imposed on our model from the Galactic center neutrinos. On the other hand, the subhalo itself may also be visible to IceCube. The DM annihilation rate within the halo can be characterized by $Q = \int \rho^2 dl d\Omega$, where ρ is the density distribution, l is the line-of-sight path length, and Ω is the integral solid angle. The annihilation rate of the subhalo for an opening angle cone of 10° is around two times higher than that of the Galactic center. It implies the previous bounds on the cross-sections will be improved by a factor of 2 in the presence of the subhalo. The favored region is, however, far below the new bounds. All in all, the current IceCube sensitivity is not able to constrain the parameter region yet.

- LZ sensitivity

As shown in the previous section, the preferred regions to account for the DAMPE bump and to reproduce the correct relic density are centered around $m_{Z'} \sim 2.6$ TeV with $g_{e\mu} \sqrt{q_\psi} \sim 0.1$. Therefore, a large part of parameter space is unaffected by the PandaX-II search. The next generation DM experiment LUX-ZEPLIN (LZ) [36, 37], however, can further improve the bound on the DM-nucleon cross-section by a factor of 50 or so, i.e., $\sigma_{\chi p}^{\text{SI}} \sim 2.4 \times 10^{-11}$ pb for TeV DM, before reaching the neutrino floor. It implies

$$g_{e\mu}^2 q_\psi \left(\frac{3058 \text{ GeV}}{m_{Z'}} \right)^2 \lesssim 1, \quad (9)$$

as indicated by the red contours in the Fig. 3. In other words, the LZ can probe a sizable part of the preferred region.

- ILC sensitivity

The LEP measurements on $e^+e^- \rightarrow e^+e^-, \mu^+\mu^-$ require the effective scale of new physics Λ (which contributes to these processes) to be above 20 TeV. Future e^+e^- colliders, such as ILC [38], FCC-ee (formerly known as TLEP [39]) and CEPC [40], can further improve the limit. The ILC, for instance, with an integrated luminosity of 1000 fb^{-1} , can probe the new physics scale Λ beyond 75 TeV [38, 41] via the process $e^+e^- \rightarrow \mu^+\mu^-$, leading to the bound $m_{Z'}/g_{e\mu} \gtrsim 21 \text{ TeV}$. The precise value of the lower bound depends on systematic uncertainties and the polarization of the electron and positron beams at the ILC.

As shown in Fig. 3, the combination of ILC and LZ projected sensitivities can disfavor a large region of the parameter space. Assuming ILC and LZ find no evidence of new physics, only the resonance region ($2m_\psi \approx m_{Z'}$) remains viable.

V. CONCLUSION

In this work, we propose a simple $U(1)_{e\mu}$ flavored neutrino mass model inspired by the DAMPE $e^+ + e^-$ excess at energies around 1.4 TeV [2]. The first two generations of leptons are charged under $U(1)_{e\mu}$ while the third one is neutral. After $U(1)_{e\mu}$ and electroweak symmetry breaking, the right-handed neutrino Majorana mass matrix is featureless, while the neutrino Dirac mass matrix is diagonal in the flavor basis. The observed neutrino masses and mixing angles can hence be easily realized via the Type-I seesaw mechanism.

The DM particle, a $U(1)_{e\mu}$ -charged vector fermion ψ , annihilates into electrons, muons and neutrinos. To account for the DAMPE excess, a local DM subhalo with a mass of $M_{\text{sub}} = 1.25 \times 10^6 M_\odot$ at a distance of 0.1 kpc from the Earth is needed. CREs lose energy so quickly on the way towards the Earth that they mostly have to come from a nearby area. The preferred parameter region is centered around $(m_\psi, m_{Z'}) \sim (1.5, 2.6) \text{ TeV}$ with $\langle \sigma_{v,\text{rel}} \rangle \sim 10^{-25} \text{ cm}^3 \text{ s}^{-1}$. We have scrutinized constraints from indirect searches (Fermi-LAT and IceCube), direct DM searches and LEP. Interestingly, a significant portion of the preferred parameter space is within the reach of the next generation lepton colliders and DM direct detection experiments.

Acknowledgments

This work is supported in part by the National Key Research and Development Program of China (No. 2016YFA0400200), the National Natural Science Foundation of China (Nos. 11525313, 11722328), and the 100 Talents Program of Chinese Academy of Sciences. WCH is supported by Danish Council for Independent Research Grant DFF-6108-00623. The CP3-Origins centre is partially funded by the Danish National Research Foundation, grant number DNRF90.

-
- [1] DAMPE, J. Chang *et al.*, *Astropart. Phys.* **95**, 6 (2017), 1706.08453.
 - [2] DAMPE, G. Ambrosi *et al.*, (2017), 1711.10981.
 - [3] X. G. He, G. C. Joshi, H. Lew, and R. R. Volkas, *Phys. Rev.* **D43**, 22 (1991).
 - [4] R. Foot, *Mod. Phys. Lett.* **A6**, 527 (1991).
 - [5] X.-G. He, G. C. Joshi, H. Lew, and R. R. Volkas, *Phys. Rev.* **D44**, 2118 (1991).
 - [6] J. Heeck and W. Rodejohann, *Phys. Rev.* **D84**, 075007 (2011), 1107.5238.
 - [7] S. Baek, H. Okada, and K. Yagyu, *JHEP* **04**, 049 (2015), 1501.01530.
 - [8] A. Biswas, S. Choubey, and S. Khan, *JHEP* **09**, 147 (2016), 1608.04194.
 - [9] W. Altmannshofer, S. Gori, M. Pospelov, and I. Yavin, *Phys. Rev.* **D89**, 095033 (2014), 1403.1269.
 - [10] J. Heeck, M. Holthausen, W. Rodejohann, and Y. Shimizu, *Nucl. Phys.* **B896**, 281 (2015), 1412.3671.
 - [11] A. Crivellin, G. D'Ambrosio, and J. Heeck, *Phys. Rev. Lett.* **114**, 151801 (2015), 1501.00993.
 - [12] A. Crivellin, G. D'Ambrosio, and J. Heeck, *Phys. Rev.* **D91**, 075006 (2015), 1503.03477.
 - [13] X.-J. Bi, X.-G. He, and Q. Yuan, *Phys. Lett.* **B678**, 168 (2009), 0903.0122.
 - [14] L. Gao, S. D. M. White, A. Jenkins, F. Stoehr, and V. Springel, *Mon. Not. Roy. Astron. Soc.* **355**, 819 (2004), astro-ph/0404589.
 - [15] J. Diemand, B. Moore, and J. Stadel, *Nature* **433**, 389 (2005), astro-ph/0501589.
 - [16] Fermi-LAT, S. Abdollahi *et al.*, *Phys. Rev.* **D95**, 082007 (2017), 1704.07195.
 - [17] J. F. Navarro, C. S. Frenk, and S. D. M. White, *Astrophys. J.* **490**, 493 (1997), astro-ph/9611107.
 - [18] V. Springel *et al.*, *Mon. Not. Roy. Astron. Soc.* **391**, 1685 (2008), 0809.0898.
 - [19] Q. Yuan *et al.*, (2017), 1711.10989.
 - [20] A. M. Atayan, F. A. Aharonian, and H. J. Volk, *Phys. Rev.* **D52**, 3265 (1995).
 - [21] O. Adriani *et al.*, *Phys. Rev. Lett.* **119**, 181101 (2017).
 - [22] Planck, P. A. R. Ade *et al.*, *Astron. Astrophys.* **594**, A13 (2016), 1502.01589.

- [23] SLD Electroweak Group, SLD Heavy Flavor Group, DELPHI, LEP, ALEPH, OPAL, LEP Electroweak Working Group, L3, t. S. Electroweak, (2003), hep-ex/0312023.
- [24] J. Kopp, V. Niro, T. Schwetz, and J. Zupan, Phys. Rev. **D80**, 083502 (2009), 0907.3159.
- [25] W.-C. Huang, A. Urbano, and W. Xue, JCAP **1404**, 020 (2014), 1310.7609.
- [26] F. D'Eramo, B. J. Kavanagh, and P. Panci, Phys. Lett. **B771**, 339 (2017), 1702.00016.
- [27] LUX, D. S. Akerib *et al.*, Phys. Rev. Lett. **118**, 021303 (2017), 1608.07648.
- [28] PandaX-II, X. Cui *et al.*, Phys. Rev. Lett. **119**, 181302 (2017), 1708.06917.
- [29] XENON, E. Aprile *et al.*, (2017), 1705.06655.
- [30] F. Feroz, M. P. Hobson, and M. Bridges, Mon. Not. Roy. Astron. Soc. **398**, 1601 (2009), 0809.3437.
- [31] L. Bergstrom, T. Bringmann, M. Eriksson, and M. Gustafsson, Phys. Rev. Lett. **94**, 131301 (2005), astro-ph/0410359.
- [32] Fermi-LAT, M. Ackermann *et al.*, Astrophys. J. **799**, 86 (2015), 1410.3696.
- [33] Fermi-LAT, M. Ackermann *et al.*, Astrophys. J. **750**, 3 (2012), 1202.4039.
- [34] CTA Consortium, M. Actis *et al.*, Exper. Astron. **32**, 193 (2011), 1008.3703.
- [35] IceCube, M. G. Aartsen *et al.*, Eur. Phys. J. **C77**, 627 (2017), 1705.08103.
- [36] D. C. Malling *et al.*, (2011), 1110.0103.
- [37] P. Cushman *et al.*, Working Group Report: WIMP Dark Matter Direct Detection, in *Proceedings, 2013 Community Summer Study on the Future of U.S. Particle Physics: Snowmass on the Mississippi (CSS2013): Minneapolis, MN, USA, July 29-August 6, 2013*, 2013, 1310.8327.
- [38] H. Baer *et al.*, (2013), 1306.6352.
- [39] TLEP Design Study Working Group, M. Bicer *et al.*, JHEP **01**, 164 (2014), 1308.6176.
- [40] CEPC-SPPC Study Group, M. Ahmad *et al.*, (2015), IHEP-CEPC-DR-2015-01, IHEP-TH-2015-01, IHEP-EP-2015-01.
- [41] S. Riemann, Fermion pair production at a linear collider: A Sensitive tool for new physics searches, in *2nd Workshop of the 2nd Joint ECFA/DESY Study on Physics and Detectors for a Linear Electron Positron Collider (28-30 June, Lund, Sweden)*, pp. 1451–1468, 2001.